J Mater Sci (2018) 53:2956–2964

Metals

Extraordinary creep relaxation time in a La-based metallic glass

M. Zhang[1,2,*], Y. Chen[2,3], D. Wei[2,3], and L. H. Dai[2,3,*]

[1] *Institute of Advanced Wear & Corrosion Resistant and Functional Materials, Jinan University, Guangzhou 510632, China*
[2] *State Key Laboratory of Nonlinear Mechanics, Institute of Mechanics, Chinese Academy of Sciences, Beijing 100190, China*
[3] *School of Engineering Sciences, University of Chinese Academy of Sciences, Beijing 100049, China*

Received: 12 August 2017
Accepted: 16 October 2017
Published online:
20 October 2017

ABSTRACT

The structural relaxation times of metallic glasses (MGs) are generally believed to decrease with increasing flow rate, also known as shear thinning. In this work, an extraordinary loading rate-independent creep relaxation time, in contrast to the decreasing Maxwell relaxation time with increasing loading rate, is observed for a La-based MG with pronounced Johari–Goldstein relaxation under nanoindentation. The Johari–Goldstein relaxation in the flow of MGs is suggested to be a form of local Newtonian flow and may be not crucial in shear thinning, whereas the main α relaxation is proposed to predominate in the shear thinning of MGs, based on the disparity between the creep relaxation time and the Maxwell relaxation time. These results improve the current understandings on the structural relaxation and its role in the shear thinning and plastic deformation of MGs.

Introduction

In plastic deformation, the structural relaxation times of metallic glasses (MGs) generally decrease with increasing flow rate [1], i.e., shear thinning. Although this shear thinning phenomenon is crucial to improving the limited plasticity of MGs [2] which determines the prospective application of these new species of metallic materials, the relevant plastic deformation mechanisms remain less well understood [3–5]. Recently, to explore the plastic deformation mechanisms of MGs, nanoindentation creep has been widely used to extract important information on the structural relaxation times during the plastic flow of MGs [6–11]. In nanoindentation tests, the deformation state of MGs beneath the indenter is highly dependent on the loading rates adopted [12], i.e., loading rate sensitive. In nanoindentation creep, the load-hold stage of the indentation program actually functions as a "deformation frozen" technique and captures the creep behavior of the in situ deformation state of MGs beneath the indenter. Therefore, the relaxation times in nanoindentation creep may serve as an indicator of the viscosity of MGs beneath the indenter deformed at different loading rates. Hence, unlike usual creep

Address correspondence to E-mail: m.zhangiwrm@jnu.edu.cn; lhdai@lnm.imech.ac.cn

DOI 10.1007/s10853-017-1725-y

tests, the creep under nanoindentation enables the investigation on the creep of the in situ plastic deformation state of MGs, which provides an important approach to examining the structural relaxation times, shear thinning mechanisms, as well as the plastic deformation mechanisms in MGs.

On the other hand, in the plastic deformation mechanisms of MGs, Johari–Goldstein (JG) relaxation [13] which is recognized as the precursor of the main α relaxation has been related to the structural defects [14] and the extraordinary plasticity of MGs [15]. To clarify the correlation between plasticity and structural relaxation of MGs, the nature of JG relaxation in MGs has been pursued with great efforts [16–18]. However, the complicated roles played by the JG relaxation and the main α relaxation, respectively, in the plasticity of MGs are still under debate and arise as two hot issues in the research of MGs [14, 19]. More specifically, to our best knowledge, although very important, the correlation between structural relaxation and shear thinning which controls the shear banding instability and toughness [20] of MGs has rarely been investigated.

Previously, by using nanoindentation creep [21] as a tool to investigate the plastic deformation of MGs, direct correlation between JG relaxation and the loading rate-dependent serrated flow of MGs has been tentatively proposed. In this work, aiming at revealing the relationship between shear thinning and the structural relaxations of MGs and disclosing the role of structural relaxations in the plastic deformation of MGs, a group of three MGs with distinct JG relaxation characteristics [21] (Online Resource I) [i.e., La MG ($La_{62}Al_{14}Ag_{2.34}Ni_{10.83}Co_{10.83}$) with pronounced JG relaxation, Pd MG ($Pd_{40}Cu_{30}Ni_{10}P_{20}$) with less pronounced JG relaxation, and Zr MG ($Zr_{41.2}Ti_{13.8}Cu_{12.5}Ni_{10}Be_{22.5}$) with no pronounced JG relaxation] are selected for nanoindentation creep. It has been found that the effect of residual stress which stems from the rapid cooling process during the fabrication of MGs may remarkably alternate the deformation behaviors of MGs and affect the nanoindentation creep tests [7]. Thus, following the method in Ref. [7], the selected three MGs were annealed for 48 h at the specific temperature $0.7T_g$ (T_g is the glass transition temperature) prior to nanoindentation creep to eliminate the effects of residual stress. As a result, an extraordinary loading rate-independent creep relaxation time for the La-based MG with pronounced Johari–Goldstein relaxation is observed. Based on this extraordinary creep relaxation time, the role of JG relaxation in the plastic deformation of MG is rationalized and a probable explanation for the relationship between shear thinning and the structural relaxations of MGs is proposed.

Materials and methods

Alloy sheets of a size of 2 mm × 30 mm × 40 mm are prepared by copper mold casting under a Ti-gettered Ar atmosphere from master alloys of the typical nominal composition: La ($La_{62}Al_{14}Ag_{2.34}Ni_{10.83}Co_{10.83}$), Pd ($Pd_{40}Cu_{30}Ni_{10}P_{20}$), and Zr ($Zr_{41.2}Ti_{13.8}Cu_{12.5}Ni_{10}Be_{22.5}$). The glassy structure of the prepared alloy is verified by X-ray diffraction (XRD, Smartlab-9) and differential scanning calorimeter (DSC, Netzsch DSC STZ 449 F3). To rule out the effect of residual stresses, the prepared alloys were annealed at $0.7T_g$ for 48 h. Before nanoindentation, the samples were carefully polished to a mirror finish. Nanoindentation tests are conducted on an Agilent Nano Indenter G200 with a Berkovich diamond tip. Load control mode and a group of loading rates $\dot{P}$: 0.33, 1.32, 13.2, and 70 mN s^{-1} are selected. In order to characterize the creep of the in situ flow state of MGs during plastic deformation at different loading rates, a reasonable transient creep time of 10 s is selected [22]. As noted in the literature [23], the thermal drift arising from the fluctuation of room temperature would impair the reliability of the observed results. Here, the choice of a creep time of 10 s is also in favor of reducing the effects of thermal drift during the load-hold stage. As shown in Fig. 1,

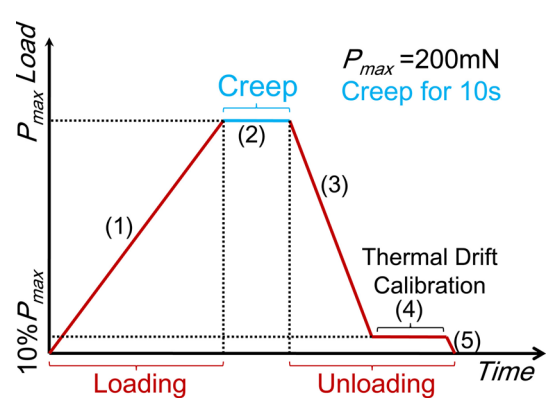

Figure 1 Schematic illustration for the experimental setup in nanoindentation creep.

the indentation program is composed by the following stages: (1) load to a maximum force P_{max} of 200 mN at a constant $\dot{P}$; (2) hold the load for 10 s at the maximum force P_{max} for creep; (3) unload to 10% of the maximum force at a rate of 10 mN s^{-1}; (4) hold the load for 10 s to perform thermal drift calibration; and (5) unload completely. To guarantee the reliability of the load (P)–displacement (h) curve, each test is repeated seven times. The details of load (P)–displacement (h) curves can be found in Online Resource II. Via continuous stiffness method tests, the mechanical rejuvenation effect induced by mechanical polishing is proved to exist in a layer of about 50 nm in thickness on the polished surface of the three MGs (Online Resource III). Therefore, the creep tests in the present work reflect the mechanical properties of the annealed sample, rather than that of the mechanically rejuvenated thin layer induced by mechanical polishing.

Results

To compare the creep behaviors of the in situ plastic deformation state of the three MGs with each other, Fig. 2a–c shows the creep curves of the annealed La, Pd, and Zr MGs during the load-hold stage in nanoindentation achieved at different loading rates. The solid points are experimental results, and the solid lines are the numerical fits. It is noted that the creep displacement for all the tests approximately saturates after a load-hold period of 10 s, indicating a proper choice of the creep time [22]. With increasing loading rate $\dot{P}$, the creep displacements during the load-hold stage increase for all the three MGs. This phenomenon may be attributed to the decreasing viscosity of each MG in flow with increasing $\dot{P}$, i.e., shear thinning. The different total creep displacements for the three MGs might also be attributed to their different in situ viscosities. To examine the creep dynamics during the plastic flow of the three MGs at different loading rates, the curves are fitted with the Kohlrausch–Williams–Watts (KWW) equation [24]: $h_c = h_0(1 - \exp(-(t/\tau_c)^{\beta}))$, for the explicit meaning of the fitting parameters, where h_c is the time-dependent creep displacement; h_0 is the total creep displacement; τ_c is the creep relaxation time; and β is the stretching exponent representing the deviation of the creep behavior from the exponential process [25]. It can be seen that all the experimental results exhibit good agreements with the KWW fits, suggesting the applicability of KWW equation to the creep of MGs.

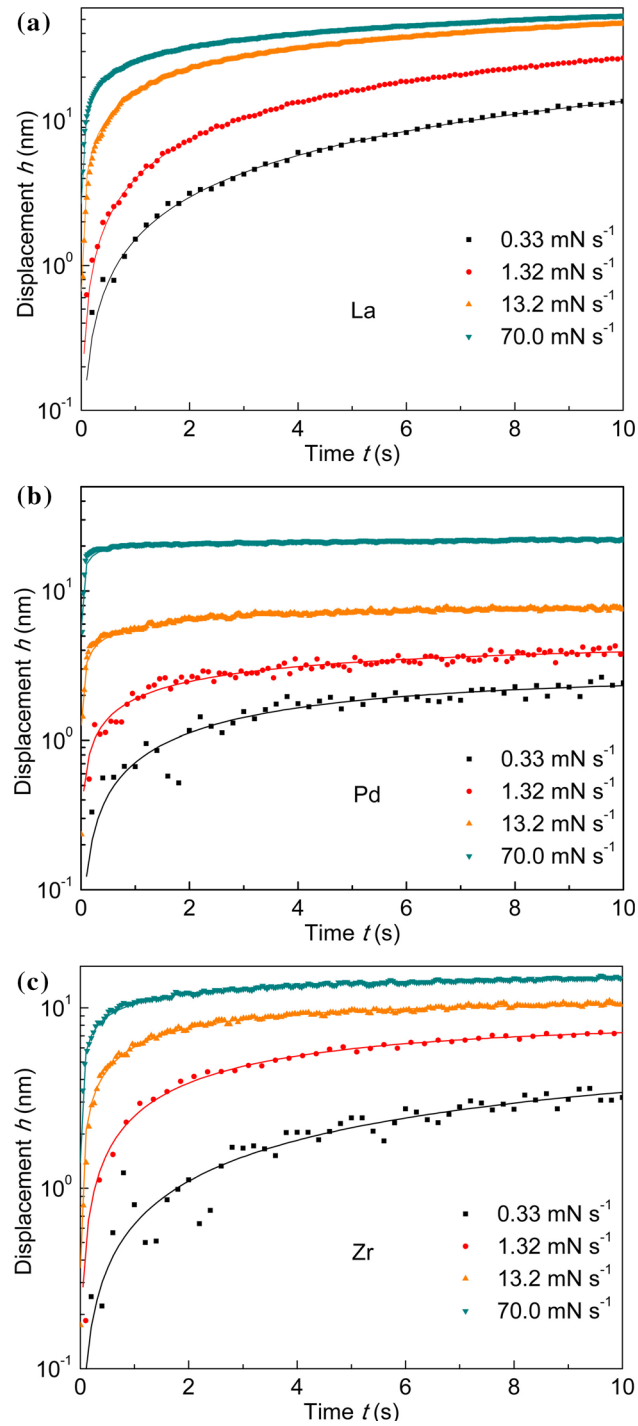

Figure 2 Displacement (h)–time (t) curves of the annealed La (**a**), Pd (**b**), and Zr (**c**) metallic glasses of the creep flow during the load-hold stage of nanoindentation. Solid lines are the Kohlrausch–Williams–Watts (KWW) equation fits.

Figure 3 shows the fitted stretching exponent β and creep relaxation time τ_c of the annealed La, Pd, and Zr MGs. The lines are drawn as eye guides. Firstly, Fig. 3a shows that the stretching exponent β for the three MGs decreases consistently from $\sim$ 1.2 to $\sim$ 0.4 with increasing loading rate $\dot{P}$. It is noted that the fact that β exceeds 1, i.e., the compressed exponential dynamics, is proposed to be due to the effect of internal atomic level stress which accelerates the relaxation process [26]. The fact that $\beta<1$ indicates a stretched exponential creep behavior and suggests that the activation energies of the structural defects of the three MGs in flow becomes non-uniform and follows a broader distribution [25] at increasing $\dot{P}$. The consistence of the decreasing of β indicates that the three MGs exhibit similar rheological dynamics under nanoindentation creep, where the distribution of the activation energies of structural defects evolves similarly with increasing $\dot{P}$. Although the variation of the stretching exponent β for the three MGs at different loading rates is also an important issue, to concentrate on the subject of the current work, i.e., shear thinning, here we focus on the creep relaxation times. The discussion on the stretching exponent β is left for future study where extensive investigation on the temperature-dependent nanoindentation creep behavior is crucial [27], since the activation energies of the structural defects of MGs are involved. It can be found in Fig. 3b that the creep relaxation time τ_c for Pd or Zr MG decreases consistently from $\sim$ 10 to $\sim$ 0.1 s, i.e., a change of two orders of magnitude, while remains $\sim$ 10 s for La MG. This result does not comply with previous works that the relaxation time generally decreases with increasing flow rate [3, 28–30] and conflicts with the common belief on the shear thinning of amorphous materials [31–33]. Compared to Zr and Pd MGs, this loading rate-independent τ_c of La MG is not likely due to its relatively low T_g, because *a relatively higher test temperature of the La MG would lead to faster creep, rather than a longer creep relaxation time*. On the other hand, the MGs during plastic flow are actually in a supercooled liquid state [34] which also makes the effect of T_g less relevant. To further prove this point, a Ce-based MG with much lower T_g is subjected to the same experimental procedure to show a shear thinning behavior similar to that of Zr and Pd MGs. The results will be published elsewhere. In addition, τ_c of the as-cast MGs are also shown in Fig. 3b to display similar results. Similar values of τ_c have been found in the same La MG [22] and also in other MG systems [7]. The values of τ_c again support the appropriate choice of a creep time of 10 s. It is noted that, for La MG, although the values of τ_c is slightly larger than the creep time, the good repetition of τ_c supports the reliability of the fit of the creep curve with KWW function shown in Fig. 2. The possible reason for the longer creep relaxation time at 70 mN s^{-1} for La MG is worth further studies in the future.

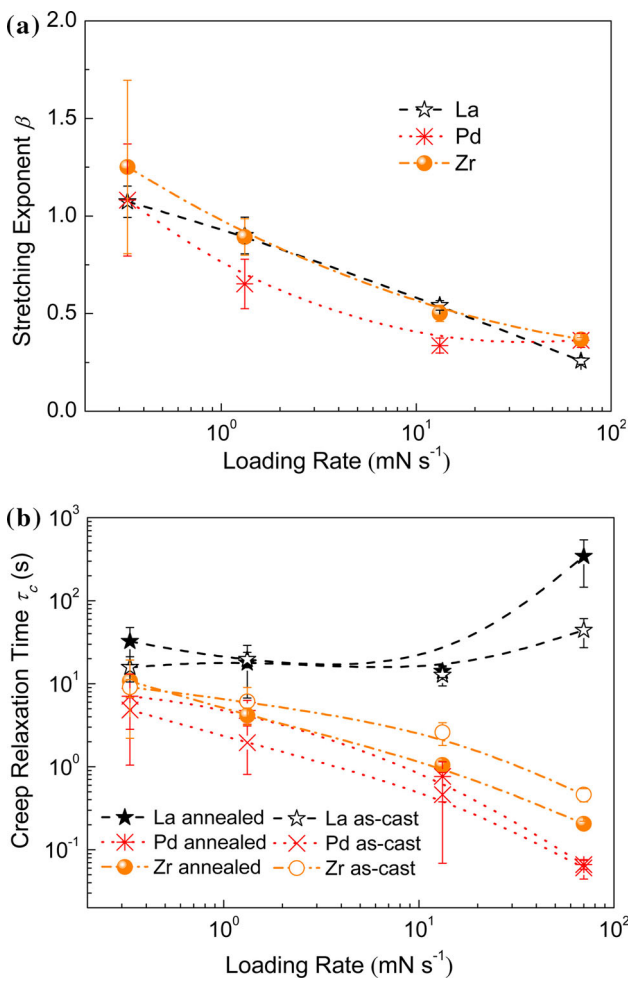

Figure 3 Stretching exponent β (**a**) and creep relaxation time τ_c (**b**) of La, Pd, and Zr metallic glasses fitted from the displacement (h)–time (t) curves. The lines are drawn as eye guides. τ_c of the as-cast MGs are also shown in (**b**).

To further understand the observed creep relaxation time τ_c, the Maxwell relaxation time $\tau_\eta = \eta_{nom}/E_r$ is also estimated for the three MGs [35], where $\eta_{nom} = \sigma/3\dot{\varepsilon} = H/9\dot{\varepsilon}$, $\dot{\varepsilon} = \dot{P}/2P_{\max}$; σ is flow stress; H is hardness; $\dot{\varepsilon}$ is strain rate; and E_r is the

nanoindentation modulus. Figure 4 shows τ_η and τ_c for the annealed La, Pd, and Zr MGs. On the physical basis, τ_c is intimately related to τ_η, since τ_η also indicates the in situ viscosity of MGs during plastic flow. This proposition is supported by the fact that τ_η of all the three MGs decrease monotonously with increasing loading rate $\dot{P}$, exhibiting a shear thinning behavior. The decreasing τ_η for the three MGs is in accordance with the increasing creep displacements h_c at increasing $\dot{P}$ shown in Fig. 2, indicating a decreasing viscosity of the MGs with increasing loading rate. It is important to see that, for Pd and Zr MGs, τ_c evolves almost consistently with τ_η. This consistence again proves the proposition that τ_η is intimately related to τ_c. However, for La MG, with a decreasing τ_η similar to that of Zr and Pd MGs, a loading rate-independent τ_c suggests an extraordinary anelastic deformation behavior and an extraordinary shear thinning mechanism in plastic deformation.

Discussion

Due to the lack of effective characterization methods to distinguish the amorphous structures of MGs with different structural relaxation characteristics, and especially due to the difficulty encountered in resolving the in situ structural evolution of MGs during plastic flow, to understand the phenomena above, a possible way is to recognize the physical process underpinning the creep relaxation time τ_c. The creep of the in situ plastic deformation state of MGs can be illustrated based on the plastic deformation mechanisms of MGs, as shown in Fig. 5a, b. Figure 5a shows the structural relaxation behaviors of MGs, which is now believed to be fundamental to the plastic deformation of MGs [36, 37]. Reversible JG relaxations (i.e., anelastic, as indicated by the small arrow) assembles into the irreversible α relaxation (i.e., plastic, as indicated by the big arrow). A consensus has been reached that the homogeneous flow of MG is naturally a stress-driven α relaxation process [36], as illustrated in Fig. 5b, noting that JG relaxations are not indicated for clarity. Accordingly, the plastic deformation of MGs (i.e., a stress-driven α relaxation) could be decomposed on the potential energy landscape into two anelastic stages. It is also noted that due to the non-affine nature of the deformation of amorphous structures, the elastic stage of the deformation is incorporated into the anelastic stage and not explicitly indicated. Namely, the configuration state of the system leaves the initial potential energy minimum and climbs onto the activation energy barrier corresponding to the first anelastic stage: the pre-plastic deformation stage, i.e., anelastic rearrangements of the amorphous structure prior to plastic deformation, and then explores the neighborhood potential energy minimum corresponding to the second anelastic stage: the post-plastic deformation stage, i.e., post-plastic anelastic rearrangements of the amorphous structure. The dot indicates the yield point of MGs in plastic deformation [36]. From this viewpoint, the creep of the in situ plastic deformation state of MG (i.e., post-plastic deformation creep) actually stems from the second anelastic deformation stage (i.e., the post-plastic deformation stage) where the system explores the neighborhood potential energy minimum via reversible JG relaxations. Since the two anelastic stages composing the plastic deformation of MGs are topologically identical to each other, τ_c can be understood as a characteristic time scale which describes the release rate of anelastic deformation into the plastically deformed state or into the initially undeformed state of MGs. Noting that both anelastic stages are an assembly of a number of JG relaxation processes, thus, τ_c is intimately related to JG relaxation and might be understood as an characteristic time scale of JG relaxation in the flow of MGs [38].

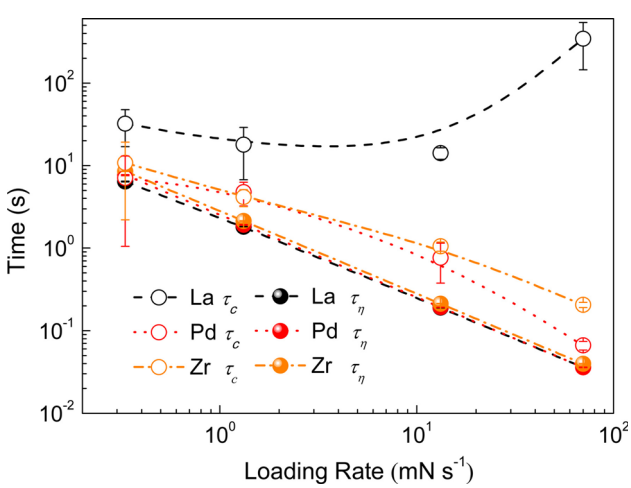

Figure 4 The Maxwell relaxation time τ_η of the annealed La, Pd, and Zr metallic glasses. The lines are drawn as eye guides. τ_c of the MGs are also shown.

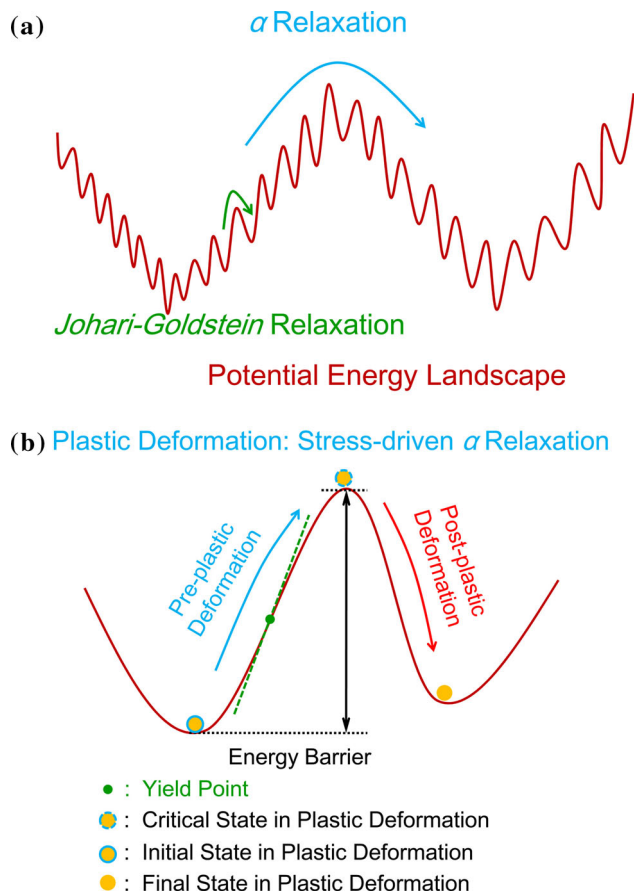

Figure 5 Schematic illustrations on the plastic deformation mechanisms of metallic glasses (MGs). **a** the relationship between α relaxation and Johari–Goldstein (JG) relaxations, where reversible JG relaxations (as indicated by the small arrow) assemble into the α relaxation (as indicated by the big arrow); **b** the flow mechanisms of MGs from the perspective of potential energy landscape: the flow of MGs (i.e., a stress-driven α relaxation) can be decomposed on the potential energy landscape into two anelastic stages, i.e., the configuration state of the system leaves the initial potential energy minimum and climbs onto the activation energy barrier corresponding to the first anelastic stage: the pre-plastic deformation stage, i.e., anelastic rearrangements of the amorphous structure prior to plastic deformation, and then explores the neighborhood potential energy minimum corresponding to the second anelastic stage: the post-plastic deformation stage, i.e., post-plastic anelastic rearrangements of the amorphous structure. The dot indicates the yield point of MGs in plastic deformation. Noting that the elastic stage of the deformation of MGs is incorporated into the anelastic stage due to the non-affine nature of the deformation of amorphous structures and that for clarity JG relaxations are not indicated.

As stated in "Results", the effect of glass transition temperature T_g is less relevant in the loading rate-independent creep relaxation time τ_c of La MG. It is also important to recall the shear thinning phenomenon that the creep displacements of La MG increases with increasing loading rate in Fig. 2a, where a decreasing viscous relaxation time (for instance, τ_η in Fig. 4) is expected. Therefore, the extraordinary loading rate-independent τ_c of La MG is probably due to its pronounced JG relaxation (i.e., an independent JG relaxation peak) compared to those of the Zr and Pd MGs, as shown in Fig. 6. Because of the independent JG relaxation peak, the pronounced JG relaxation of La MG is presumably less affected by the main α relaxation (or by τ_η, which is actually determined by the main α relaxation) and might cancel the local atomic rearrangement-induced shear dilation inside the structural defects of MGs, based on the intimate relation between structural defects and JG relaxations [15]. Hence, the JG relaxation is suggested to be a form of Newtonian flow with a constant characteristic relaxation time within the structural defects of MGs. This conclusion is supported by the increasing size of serrations (Online Resource II) of the La MG with increasing loading rate in the high loading rate regime where a decreasing size of serrations with increasing loading rate is usually observed for MGs with a similar low T_g, such as the Mg-based MG [12]. More details for the demonstration of the origin of the increasing serrations of the La MG can be found in our previous work [21]. It is important to emphasize in here that the loading rate-independent creep relaxation time τ_c of La MG is not exactly the JG relaxation time itself, but an indication of the characteristic time scale of JG relaxation in the nanoindentation creep of La MG. On the other hand, the decreasing τ_c of Pd and Zr MGs

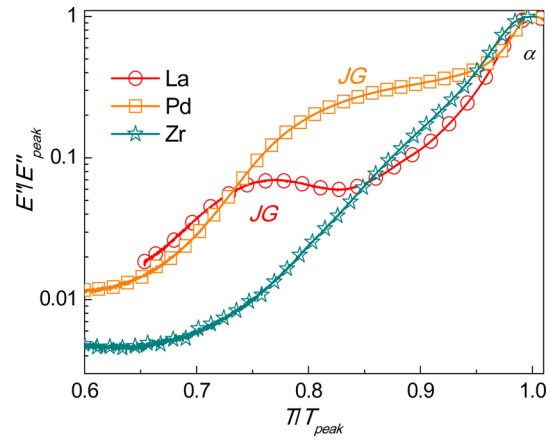

Figure 6 Johari–Goldstein (JG) relaxation and α relaxation of the La, Pd, and Zr metallic glasses.

with increasing loading rate is probably due to the absence of a pronounced JG relaxation, i.e., the absence of an independent JG relaxation peak. As shown in Fig. 6, the JG relaxation is overwhelmingly overlapped by the main α relaxation for Pd and Zr MGs, which suggests that the JG relaxation of Pd and Zr MGs might be significantly affected by the main α relaxation. This suggestion explains the consistent decreasing tendency of τ_c and τ_η of the Pd and Zr MGs, where the τ_c might be strongly affected by the τ_η which is determined by the main α relaxation.

Furthermore, the disparity between the loading rate-independent creep relaxation time τ_c and the decreasing Maxwell relaxation time τ_η of the La MG provides an important clue on the shear thinning mechanisms of MGs, which would also help to understand the relationship between α relaxation and JG relaxation [39]. The shear thinning mechanisms of supercooled liquids have been addressed previously [3], where the self-assembly of the structural defects into anisotropic fluidized bands is proposed to be crucial. The shear thinning mechanisms in wormlike micelles are also ascribed to the alignment of the micelles in flow [31], a self-assembly phenomenon resembling the anisotropic fluidized bands. Therefore, the self-assembly of typical microstructures [40] may predominate in the shear thinning mechanisms of amorphous materials. As illustrated in Fig. 5a, in the flow of MGs, JG relaxation acts as elementary flow structural defect. Hence, it is proposed that the self-assembly of the JG relaxation processes, viz. the α relaxation, may predominate in the shear thinning mechanisms, whereas the JG relaxation itself may be not crucial in shear thinning. This proposition is nicely justified by the disparity between the loading rate-independent creep relaxation time τ_c and the decreasing Maxwell relaxation time τ_η. As discussed above, the loading rate-independent τ_c is determined by the JG relaxation which is a form of local Newtonian flow and exhibits no prominent shear thinning, implying the negligible contribution of JG relaxation in shear thinning. On the other hand, the decreasing τ_η is determined by the viscosity of MGs which is actually determined by the main α relaxation and exhibits a shear thinning behavior, indicating the predominating contribution of the α relaxation in shear thinning. This proposition is supported by the observation that the viscous glassy dynamics is always determined by the α relaxation [41]. Besides, it is noted that the disparity between τ_c and τ_η is also consistent with the decoupling between diffusion and viscosity in glasses, i.e., the breakdown of the Stokes–Einstein relation [42], since that JG relaxation which determines τ_c is intimately related to the atomic diffusion of MGs [38] and that the α relaxation which determines τ_η is intimately related to viscosity. This consistence supports the reliability of our observation of a loading rate-independent creep relaxation time and in turn supports the proposition that the α relaxation predominates in the shear thinning of MGs. To further verify this proposition, future works on the issues of structural relaxation dynamics during the plastic deformation of MGs, such as the role of JG relaxation in the plastic flow of Pd and Zr MGs, are in urgent need.

Conclusions

In summary, a loading rate-independent creep relaxation time of a La-based MG with pronounced JG relaxation is observed in contrast to two other MGs of which the creep relaxation times exhibit a shear thinning behavior at increasing loading rate in nanoindentation creep. Compared to the Maxwell relaxation time, the loading rate-independent creep relaxation time of the La MG suggests that the nature of JG relaxation is a form of local Newtonian flow within the structural defects of MGs and that the self-assembly of JG relaxations, viz. α relaxation, predominates in the shear thinning mechanisms of MGs. These results would advance the current knowledge on the roles of structural relaxations in the plastic deformation mechanisms of metallic glasses, which will help to design new species of metallic glasses with excellent plasticity.

Acknowledgements

This work was financially supported by the National Nature and Science Foundation of China under Grant Nos. 11472287 and 11572324, the Key Research Program of Frontier Sciences under Grant No. QYZDJSSW-JSC011, and the Strategic Priority Research Program of the Chinese Academy of Sciences under Grant Nos. XDB22040302 and XDB22040303. M.Z. and Y.C. are also grateful for the

support of the Opening fund of State Key Laboratory of Nonlinear Mechanics (Grant No. LNM201718).

Compliance with ethical standards

Conflict of interest The authors declare no conflicts of interest.

Electronic supplementary material: The online version of this article (doi:10.1007/s10853-017-1725-y) contains supplementary material, which is available to authorized users.

References

[1] Nieh TG, Schuh C, Wadsworth J, Li Y (2002) Strain rate-dependent deformation in bulk metallic glasses. Intermetallics 10:1177–1182

[2] Schuh CA, Hufnagel T, Ramamurty U (2007) Mechanical behavior of amorphous alloys. Acta Mater 55:4067–4109

[3] Furukawa A, Kim K, Saito S, Tanaka H (2009) Anisotropic cooperative structural rearrangements in sheared supercooled liquids. Phys Rev Lett 102:016001

[4] Langer JS, Egami T (2012) Glass dynamics at high strain rates. Phys Rev E 86:011502

[5] Li N, Liu Z, Wang XY, Zhang M (2017) Vibration-accelerated activation of flow units in a Pd-based bulk metallic glass. Mater Sci Eng A Struct Mater Prop Microstruct Process 692:62–66

[6] Wei BC, Zhang TH, Li WH, Xing DM, Zhang LC, Wang YR (2005) Indentation creep behavior in Ce-based bulk metallic glasses at room temperature. Mater Trans 46:2959–2962

[7] Castellero A, Moser B, Uhlenhaut DI, Dalla Torre FH, Loffler JF (2008) Room-temperature creep and structural relaxation of Mg–Cu–Y metallic glasses. Acta Mater 56:3777–3785

[8] Huang YJ, Shen J, Chiu YL, Chen JJJ, Sun JF (2009) Indentation creep of an Fe-based bulk metallic glass. Intermetallics 17:190–194

[9] Chen YH, Huang JC, Wang L, Nieh TG (2013) Effect of residual stresses on nanoindentation creep behavior of Zr-based bulk metallic glasses. Intermetallics 41:58–62

[10] Ma Y, Ye JH, Peng GJ, Wen DH, Zhang TH (2015) Loading rate effect on the creep behavior of metallic glassy films and its correlation with the shear transformation zone. Mater Sci Eng A Struct Mater Prop Microstruct Process 622:76–81

[11] Wang C, Cao QP, Wang XD, Zhang DX, Qu SX, Jiang JZ (2017) Time-dependent shear transformation zone in thin film metallic glasses revealed by nanoindentation creep. J Alloys Compd 696:239–245

[12] Schuh CA, Lund AC, Nieh TG (2004) New regime of homogeneous flow in the deformation map of metallic glasses: elevated temperature nanoindentation experiments and mechanistic modeling. Acta Mater 52:5879–5891

[13] Johari GP, Goldstein M (1970) Viscous liquids and the glass transition. II. Secondary relaxations in glasses of rigid molecules. J Chem Phys 53:2372–2388

[14] Yu HB, Wang WH, Bai HY, Samwer K (2014) The beta-relaxation in metallic glasses. Natl Sci Rev 1:429–461

[15] Yu HB, Wang WH, Bai HY, Wu Y, Chen MW (2010) Relating activation of shear transformation zones to beta relaxations in metallic glasses. Phys Rev B 81:220201

[16] Yu HB, Samwer K, Wang WH, Bai HY (2013) Chemical influence on beta-relaxations and the formation of molecule-like metallic glasses. Nat Commun 4:2204

[17] Liu YH, Fujita T, Aji DPB, Matsuura M, Chen MW (2014) Structural origins of Johari–Goldstein relaxation in a metallic glass. Nat Commun 5:3238

[18] Zhu F, Nguyen HK, Song SX, Aji DPB, Hirata A, Wang H, Nakajima K, Chen MW (2016) Intrinsic correlation between beta-relaxation and spatial heterogeneity in a metallic glass. Nat Commun 7:11516

[19] Qiao JC, Pelletier JM (2014) Dynamic mechanical relaxation in bulk metallic glasses: a review. J Mater Sci Technol 30:523–545

[20] Jiang MQ, Dai LH (2009) On the origin of shear banding instability in metallic glasses. J Mech Phys Solids 57:1267–1292

[21] Zhang M, Wang YJ, Dai LH (2016) Understanding the serrated flow and Johari–Goldstein relaxation of metallic glasses. J Non Cryst Solids 444:23–30

[22] Liang DD, Wang XD, Ma Y, Ge K, Cao QP, Jiang JZ (2013) Decoupling of pronounced beta and alpha relaxations and related mechanical property change. J Alloys Compd 577:257–260

[23] Maier V, Merle B, Goken M, Durst K (2013) An improved long-term nanoindentation creep testing approach for studying the local deformation processes in nanocrystalline metals at room and elevated temperatures. J Mater Res 28:1177–1188

[24] Williams G, Watts DC (1970) Non-symmetrical dielectric relaxation behaviour arising from a simple empirical decay function. Trans Faraday Soc 66:80–85

[25] Wang Z, Sun BA, Bai HY, Wang WH (2014) Evolution of hidden localized flow during glass-to-liquid transition in metallic glass. Nat Commun 5:5823

[26] Ruta B, Baldi G, Monaco G, Chushkin Y (2013) Compressed correlation functions and fast aging dynamics in metallic glasses. J Chem Phys 138:054508

[27] Qiao JC, Wang Y-J, Zhao LZ, Dai LH, Crespo D, Pelletier JM, Keer LM, Yao Y (2016) Transition from stress-driven to thermally activated stress relaxation in metallic glasses. Phys Rev B 94:104203

[28] Langer JS (2012) Shear-transformation-zone theory of viscosity, diffusion, and stretched exponential relaxation in amorphous solids. Phys Rev E 85:051507

[29] Falk ML, Langer JS (1998) Dynamics of viscoplastic deformation in amorphous solids. Phys Rev E 57:7192–7205

[30] Albano F, Falk ML (2005) Shear softening and structure in a simulated three-dimensional binary glass. J Chem Phys 122:154508

[31] Forster S, Konrad M, Lindner P (2005) Shear thinning and orientational ordering of wormlike micelles. Phys Rev Lett 94:017803

[32] Dullens RPA, Bechinger C (2011) Shear thinning and local melting of colloidal crystals. Phys Rev Lett 107:138301

[33] Vazquez-Quesada A, Tanner RI, Ellero M (2016) Shear thinning of noncolloidal suspensions. Phys Rev Lett 117:108001

[34] Wang YJ, Zhang M, Liu L, Ogata S, Dai LH (2015) Universal enthalpy–entropy compensation rule for the deformation of metallic glasses. Phys. Rev B 92:174118

[35] Pan D, Inoue A, Sakurai T, Chen MW (2008) Experimental characterization of shear transformation zones for plastic flow of bulk metallic glasses. Proc Natl Acad Sci USA 105:14769–14772

[36] Harmon JS, Demetriou MD, Johnson WL, Samwer K (2007) Anelastic to plastic transition in metallic glass-forming liquids. Phys Rev Lett 99:135502

[37] Wang WH (2011) Correlation between relaxations and plastic deformation, and elastic model of flow in metallic glasses and glass-forming liquids. J Appl Phys 110:053521

[38] Yu HB, Samwer K, Wu Y, Wang WH (2012) Correlation between beta relaxation and self-diffusion of the smallest constituting atoms in metallic glasses. Phys Rev Lett 109:095508

[39] Goldstein M (2010) Communications: comparison of activation barriers for the Johari–Goldstein and alpha relaxations and its implications. J Chem Phys 132:041104

[40] Lemaitre A (2014) Structural relaxation is a scale-free process. Phys Rev Lett 113:245702

[41] Lunkenheimer P, Wehn R, Schneider U, Loidl A (2005) Glassy aging dynamics. Phys Rev Lett 95:055702

[42] Geyer U, Schneider S, Johnson WL, Qiu Y, Tombrello TA, Macht MP (1995) Atomic diffusion in the supercooled liquid and glassy states of the $Zr_{41.2}Tii_{3.8}Cu_{12.5}nN_{10}Be_{22.5}$ alloy. Phys Rev Lett 75:2364–2367